Supplementary Information:

A Self-Driven Wideband Wavelength Sensor Based on an Individual $PdTe_2$/Thin Si/$PdTe_2$ Heterojunction

Xiao-Wei Tong, [a] *Min Fan,* [a] *Chao Xie,*[*b] *Li Wang,* [c] *Hai-Bo Wang,* [a] *Qin-Qin Qian,* [a] *Shi-Bin Lu,* [a] *Lin Jin,* [a] *Zhong-Xiang Zhang*[*a]

[a] Anhui Province Key Laboratory of Simulation and Design for Electronic Information System, Hefei Normal University, Hefei, Anhui 230601, P. R. China.

[b] Industry-Education-Research Institute of Advanced Materials and Technology for Integrated Circuits, School of Electronics and Information Engineering, Anhui University, Hefei, Anhui 230601, P. R. China.

[c] School of Microelectronics, Hefei University of Technology, Hefei, Anhui 230009, P. R. China.

[*] Email: chaoxie@ahu.edu.cn; zhzhx@hfnu.edu.cn

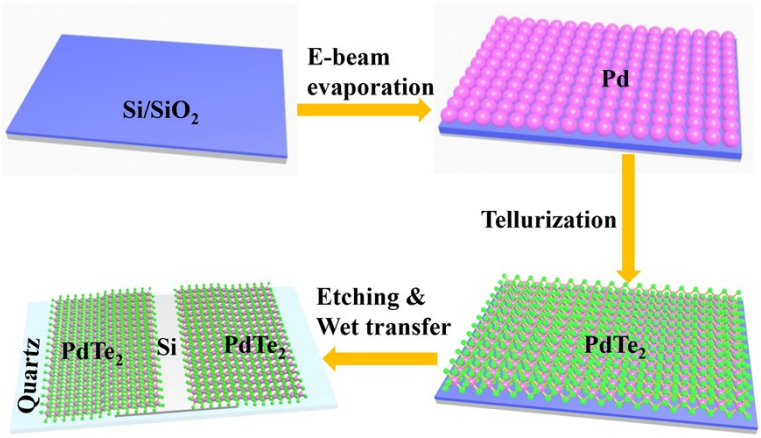

Figure S1. Schematic diagram of the procedures for synthesizing 2D $PdTe_2$ nanofilm and fabricating the designed color sensor.

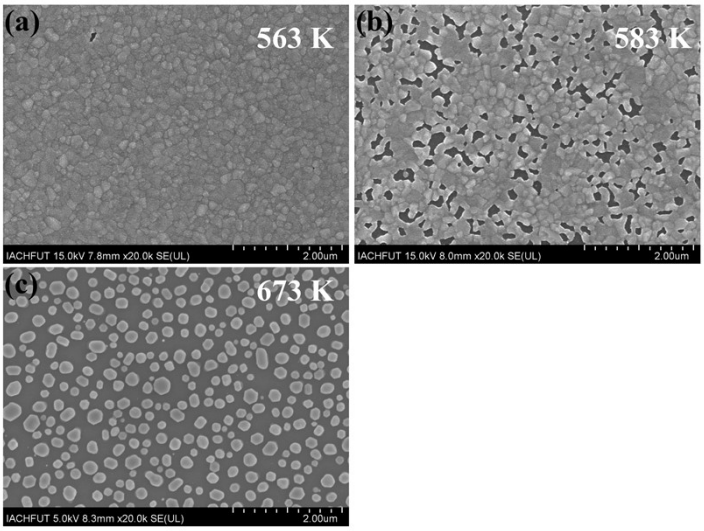

Figure S2. SEM images of the 2D PdTe2 synthesized at different temperatures of (a) 563 K, (b) 583 K and (c) 673 K.

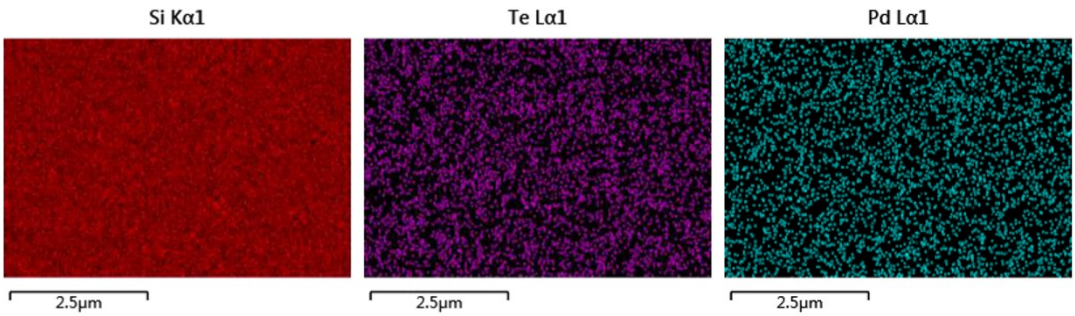

Figure S3. The corresponding EDS mapping of 2D $PdTe_2$ nanofilm on thin Si.

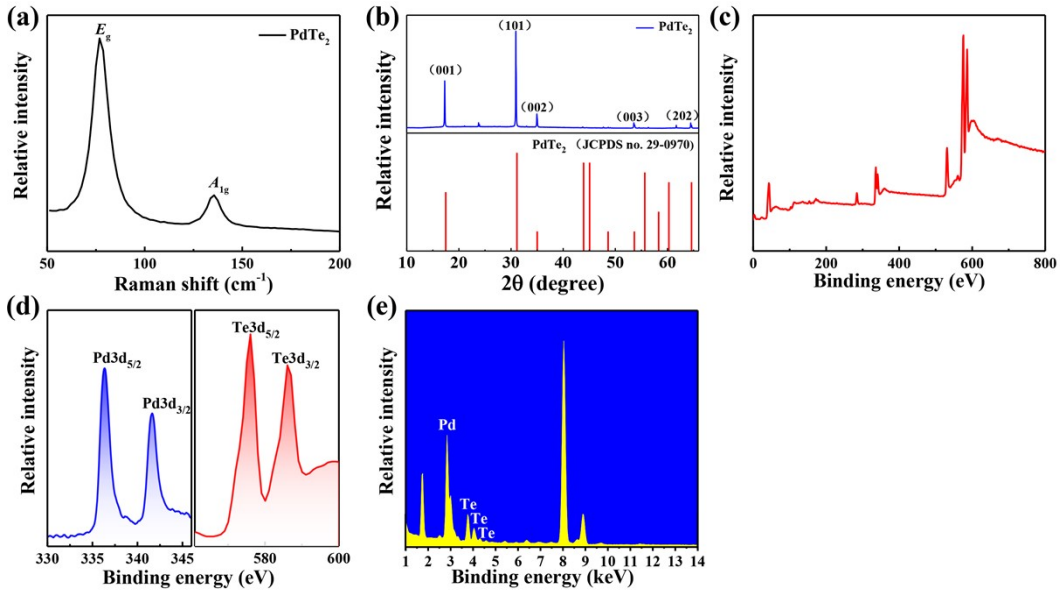

Figure S4. (a) Raman spectrum, (b) XRD pattern, (c) XPS spectrum, (d) XPS spectra of Pd 3d (left panel) and Te 3d (right panel), and (e) EDS spectrum of the as-synthesized $PdTe_2$ nanofilm.

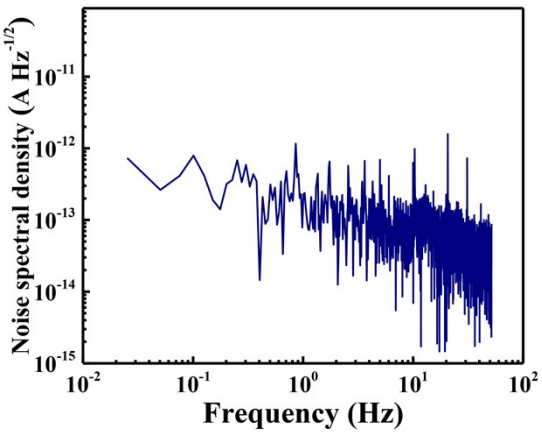

Figure S5. The noise spectral density of the $PdTe_2$/thin Si/$PdTe_2$ heterojunction.

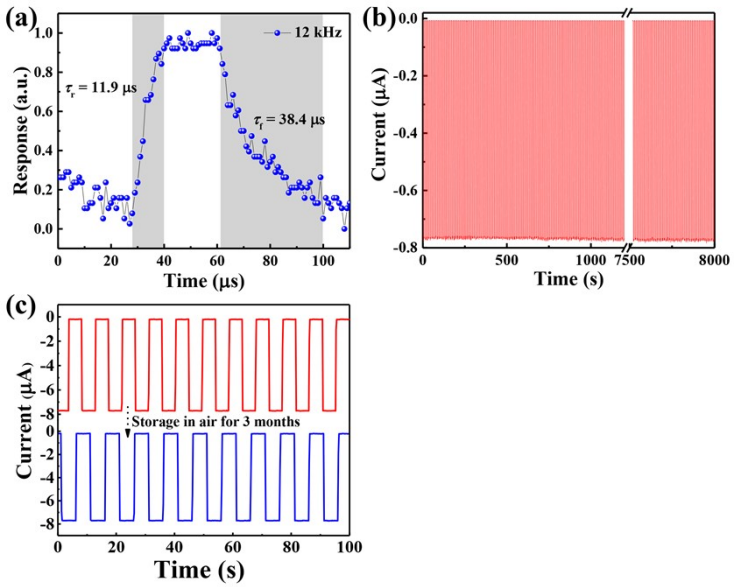

Figure S6. Transient photoresponse of the $PdTe_2$/Si/$PdTe_2$ heterojunction device (a) at light modulation frequency of 12 kHz, (b) under 730 nm light illumination over 8000 cycles of operation, and (c) before and after storage in ambient conditions for 3 months.

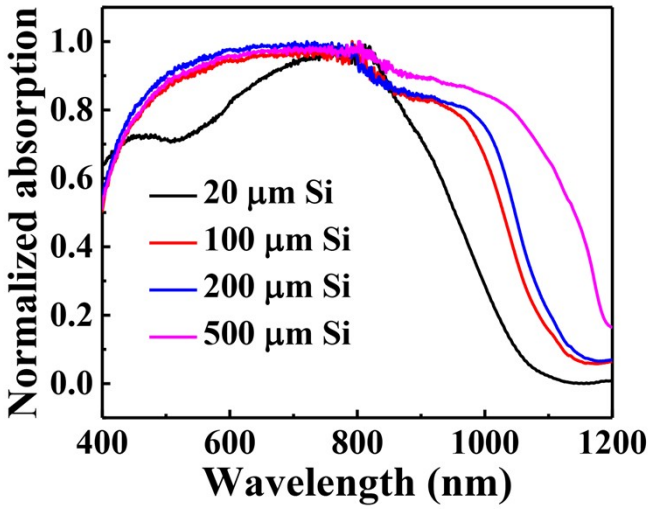

Figure S7. Optical absorption spectra of Si wafers with diverse thicknesses.

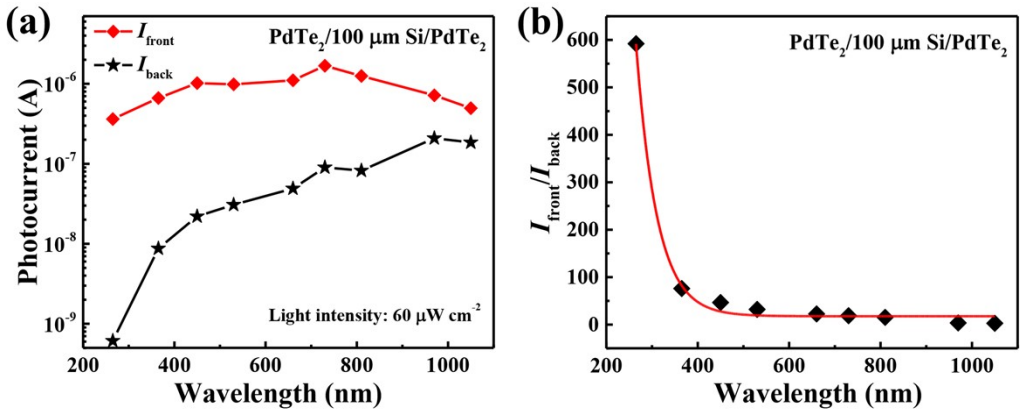

Figure S8. (a) Photocurrents at front- and back-illuminated modes and (b) photocurrent ratio *versus* light wavelength of 100 μm-thick Si device at light intensity of 60 μW cm^{-2}.

Table S1. The values of the constants of the work curve at several specific light intensities and working bias voltages.

Light intensity	Bias voltage	A	B	C	D
50 μW cm^{-2}	0 V	60.43389	104.0626	2.54829	370.8137
30 μW cm^{-2}	0 V	73.62578	114.8314	2.13944	362.4086
20 μW cm^{-2}	0 V	72.76912	112.8695	2.22853	371.5909
10 μW cm^{-2}	0 V	76.66907	120.7684	2.00986	376.5797
10 μW cm^{-2}	-0.1 V	82.0998	130.6842	1.61825	348.5703
10 μW cm^{-2}	-0.2 V	81.80273	126.3258	1.54657	349.9691
10 μW cm^{-2}	-0.3 V	81.22581	123.8618	1.59006	348.3812